A Language and Compiler for Iterative Stencil Loops

Jeremy W. Sheaffer, Gregory Faust, Salvatore Valente, Kim Hazelwood and Kevin Skadron
{jws9c, gf4ea, sv9wn, hazelwood, skadron}@cs.virginia.edu

Department of Computer Science Department, University of Virginia

***Abstract*—We present a high-level language for iterative stencil loops called *Stencil Language* (SL). Using SL, a programmer need only express the central kernel of their computation, not an entire parallel program. We have also built a translator for SL capable of translating the SL program into code for different parallel programming models. We provide an initial translation into optimized code for the C++ extensions of the CUDA programming model for NVIDIA GPUs and for multi-node CUDA distributed with MPI. Our CUDA optimizer is an extension of a previously proposed analytical model for CUDA stencil applications. Our model improves over the previous model by automatically utilizing both static and dynamic information about the application and the specific GPU environment in which the application is running. This allows the optimized version of the application to be derived without the need for the application developer to specify any execution-environment specific information. Finally, we provide results that show that the code generated from SL for CUDA is up to $2.3\times$ faster than naïve CUDA code across six applications and two generations of NVIDIA hardware.**

I. Introduction

Iterative stencil loops (ISLs) [1] are a class of loops that are commonly used in fields including numerical simulations and signal processing. ISLs compute a time varying set of values in an array. The value for each array element in each time step depends upon the value for that element and a set of nearby elements from the previous time step. The pattern of neighboring elements is called the *stencil*. This access pattern means that each element in the current time step can be calculated independently of all others. Therefore, techniques that take advantage of data parallelism are applicable to ISLs, and can often lead to dramatic speedups over serialized implementations, yet implementing parallel ISLs presents several challenges.

A typical implementation of a parallel ISL divides the array into *tiles* and assigns one or more tiles to each processor. A complication of this technique is that elements near the edge of a tile may reside in a tile assigned to another processor; therefore, a certain amount of data sharing between otherwise disjoint tiles is required. Furthermore, on architectures with a high communication cost, an optimal ISL implementation allows each processor to calculate several time steps on its tiles before requiring communication.

To accommodate this communication delay, disjoint tiles must overlap. The amount of overlap increases with the number of time steps between communication events. Additionally, values of array elements in the overlapping region must be redundantly calculated because each processor needs the boundary values locally for intermediate time steps. The correct number of time steps to allow between processor synchronization is therefore a trade-off between the cost of synchronization and the associated data exchange, and the number of redundant values that are calculated.

These trade-offs are poorly understood and are highly architecture dependent. They are particularly challenging on new accelerator processors with novel memory hierarchies and synchronization support; GPUs are a prominent example, having attracted great interest for general-purpose engineering and scientific computing due to their high data-parallel throughput and low cost.

What is needed is a way for users to express ISL computation in a way that allows them to focus on their application rather than the parallel optimization techniques needed for performance. In this paper, we discuss our efforts to provide such a system. Our contributions are as follows:

- We have implemented SL, a formal, high-level language in which a programmer can describe an ISL computation. By design, a description written in the language must include all of the information necessary to calculate the correct results, and none of the information that would tie its performance to a particular architecture.
- We have created a front-end compiler for SL that can easily be extended with multiple back-ends. Based on a single source file, produces code for CUDA [2], [3], OpenMP [4] and MPI [5].
- Our CUDA code optimizer transparently calculates the optimal tile size and time steps between synchronizations, and takes advantage of scratchpad memory. It extends the analytical model proposed by Meng and Skadron [6].
- Our system automatically collects all the necessary application specific and execution environment information needed by the model. Some is derived statically from the SL program, and the rest is derived dynamically at runtime.
- Dynamic acquisition of the execution environment information allows the generated code to calculate good values on a variety of GPU cards. We demonstrate this capability by reporting results on both the Tesla and

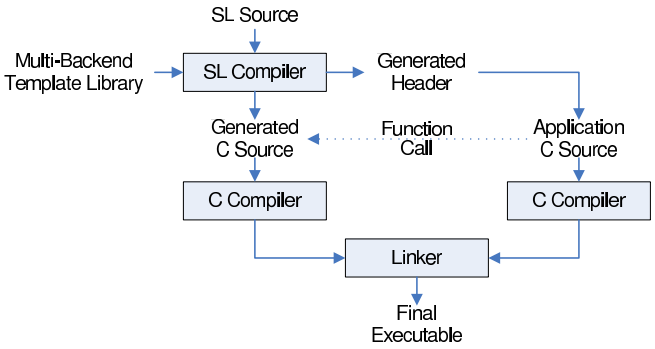

Figure 1. SL System Diagram showing information flow in SL. The SL source is combined by the SL compiler with the appropriate optimized back-end template. The resultant generated subroutine for the ISL calculation is called by the rest of the user's application code.

Fermi architectures.

II. SL System Organization

Figure 1 shows the system organization and information flow of the SL compiler. The application programmer specifies an ISL computation in an SL source file. The remainder of their application is specified in C or C++. In a simple scenario, the application code configures the array upon which the ISL will operate and calls the code generated by the SL compiler to do the ISL computation. The results of the ISL computation can then be used by the application. The SL compiler generates a C Header File for inclusion in the application code to declare the signature of ISL subroutines.

Figure 1 shows the general system organization. The SL compiler takes in two sources of information: the SL program and and SL system template that includes hand optimized implementations of the general structure of an ISL computation for various runtime environments. The templates are written by the SL system developers, not the SL user. Based on the user specified target environment, the SL compiler selects the appropriate library template and modifies it to implement the user's stencil calculation. The SL compiler produces program source as output, essentially a source-to-source process, which is linked with the user's application source into a final executable.

Many scientific applications require multiple ISL computations in a pipeline. This usage scenario is supported by our system. Each ISL computation is specified in its own SL source file. The user's application code can then call the generated subroutine for each ISL computation as needed.

III. Iterative Stencil Loops: Terms & Background

Iterative stencil loops [1] are a class of loops, commonly used in numerical simulations and signal processing, which typically operate on matrices with one, two, or three dimensions. An ISL calculation takes an input matrix m_{in} and produces an output matrix m_{out}. The calculation has the following properties:

1) m_{in} and m_{out} have the same number of dimensions and are the same size.
2) Each value in m_{out} is calculated independently of each other value in m_{out}.
3) There is a single function which is used to calculate each value in m_{out} regardless of the coordinates of the value.

For example, suppose m_{in} is a two-dimensional matrix, and the stencil calculation is defined as "$m_{out}[x, y] =$ the average of the north, south, east, and west neighbors of $m_{in}[x, y]$". Then this function will be calculated for every cell in m_{out}.

The *stencil* is the set of cells in the input matrix that is used in the stencil calculation, relative to the coordinates of the cell that is being calculated. In the above example, the stencil is a set of four cells: the north, south, east, and west neighbors.

The process of calculating a complete output matrix is called an *iteration* or a *time step*. At the end of an iteration, the output matrix m_{out} is used as the input matrix to the next iteration. This loop can continue for as long as necessary. Some iterative stencil loops are defined to run for a predetermined number of time steps, while others are defined to run until the values converge. Both cases are handled by SL.

Stencil calculations are data parallel. Since each value in a time step is calculated independently, the values can be calculated in any order. If the matrix has n cells and the computer has k *processing elements* (PEs) available, then each processor only needs to calculate a block of size n/k. This partitioning of the matrices among multiple processors is called *tiling*, and the block calculated by a PE is called a *tile*.

When a PE calculates a given tile for many iterations, that PE can take advantage of both spatial locality and temporal locality.

- **Spatial locality:** As a general rule, stencil calculations use each input value multiple times. For example, given a stencil defined as a cell's left and right neighbors, when a PE calculates the cell value at $x = i$, it reads the value of the right neighbor at $x = i + 1$. When it calculates the cell value at $x = i + 2$, it reads the left neighbor, the value at $x = i + 1$ again. Thus, a PE can optimize computation by keeping input values in a local cache or scratchpad.
- **Temporal locality:** If a PE generates an output value during iteration t, then that PE can use that value as an input value during iteration $t + 1$.

Unfortunately, if each PE is given only those array values that fall within its tile size, cells along the boundary of the tile will not find all of their inputs in the local cache. These cells must obtain some of their inputs from array values assigned to other PEs. In the example above, the cell in the bottom left corner of a tile will require values for both its south and west neighbors from neighboring tiles. The region of data surrounding a tile that is needed from adjacent tiles is called its *ghost zone* or GZ.

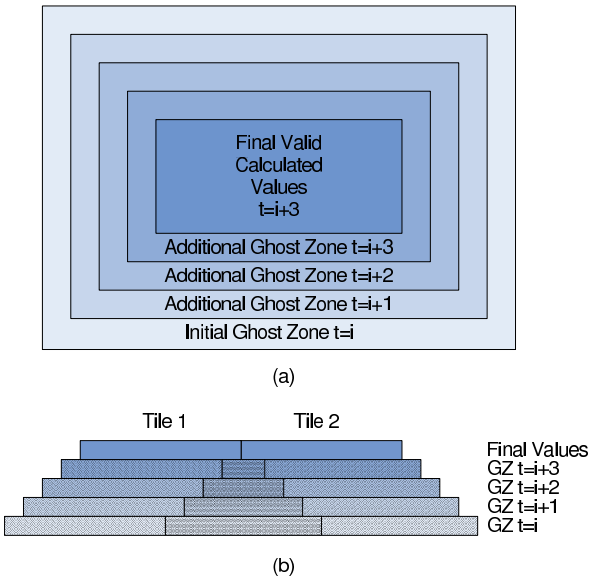

Figure 2. (a) For a single tile in a 2D matrix, the number of valid calculated values decreases with each additional time interval between synchronization events. After 4 time steps, only the inner most rectangle of n values are valid. (b) Two adjacent tiles shown from the plane of the 2D array with time in the vertical dimension. In the first time step (bottom) there is substantial overlap in the ghost zones in order to have the resultant valid values abut after 4 time steps (top).

In order to take advantage of temporal locality, each PE may want to compute more than one time interval with the array values it has stored locally; however, at each successive time interval, more values at the periphery of the PEs local store become stale. For example, consider the 2D tile computation shown in Figure 2(a). It shows the shrinking number of valid values calculated in a tile over four time intervals. In the first time interval, i, with a stencil size of one, the PE will require a GZ of size one all around the periphery of the tile. However, in calculating the second time interval $i+1$, the values in the original GZ are still from time i and are now out of date. Therefore, the PE is only able to calculate a smaller number of valid values, and the size of the GZ has expanded by the size of the stencil on all sides of the tile. In the diagram, this progression of stale values and expanding GZs will continue inward through time interval $t + 3$, after which only the inner most rectangle will have valid values.

Figure 2(b) shows the overlap in GZs between two adjacent tiles for the same computation over four time intervals with time in the vertical dimension. Each PE must start with GZ size four in order to have valid values computed for the resultant tiles cover the entire input array. Because the size of the area of valid values for a PE shrink with time in this way, the number of time intervals each PE calculates between synchronization events is called the *pyramid height* or PH of the ISL. In general, the size of the required GZ is equal to twice the size of the stencil times the PH. In addition, the values for cells in all but the initial GZ are redundantly calculated by adjacent PEs.

```
NumDimensions 2
StencilSize (1, 1)
DataType float
FunctionName runHotspot

ScalarVariables (
  float Rx, float Ry, float Rz
}
CellValue {
  float pvalue, value, term1, term2, term3, sum;
  pvalue = read(y * input_size.x + x);
  value = get(0, 0);
  term1 = (get(0, 1) + get(0, -1) - value) / Ry;
  term2 = (get(1, 0) + get(-1, 0) - value) / Rx;
  term3 = (80.0 - value) / Rz;
  sum = pvalue + term1 + term2 + term3;
  return(value + sum);
}
EdgeValue {
  return value;
}
```

Figure 3. The `hotspot.sl` stencil language file. This example shows a 2D stencil calculation where each cell value is based on the values of that cell's immediate neighbors. The read-only data is interpreted as a 2D matrix in row-major order which indicates that some areas of the chip inherently run hotter then other areas.

As a result of the required data exchange between PEs, ISL algorithms may spend considerable time stalled due to communication and synchronization delays. Because synchronization events can have high latencies, it is often better to reduce the number of synchronizations between PEs by increasing the PH and therefore the size of the GZ. As we have seen, larger GZs result in larger data exchanges at each synchronization and more redundant calculations; therefore, the choice of the optimal PH for an ISL involves a trade-off between these two competing costs and benefits. The performance of ISLs depends critically upon the correct choice.

There have been several attempts to optimize these trade offs, such as the study by Meng and Skadron [6] which examines the problem of writing efficient ISL code in CUDA. They define a mathematical model to calculate the optimal PH for an ISL targeted for NVIDIA GPUs. We have built upon the results of that study, and have fully automated that optimization process in our SL compiler.

IV. Stencil Language Description

Figure 3 shows an SL description of the "HotSpot" calculation. This code calculates temperature across a two-dimensional microchip where the current state is a function of the previous state, the edge values, and a 2D read-only "power usage" matrix. We will examine the various aspects of this example in turn.

A. Syntax

A stencil language file is a text file that contains a set of key-value pairs. A key is an alphanumeric string. A value can be:

- an integer

- a name comprised of alphanumeric and underscore characters
- a list of names, inside parentheses, separated by commas
- a block of code inside of curly braces

We do not provide a grammar for SL as the key-value pairs are sufficiently simple (constituting a regular language) as to obviate its need. Technically, SL is only scanned, not parsed. On a scan error, the system prints an error message and aborts. Other errors will be caught by the backend compiler after the system makes substitutions into the backend template; with the backend code used in the prototype, *#line* directives are inserted into generated source to aid the user with both compile- and run-time errors.

B. Content

The currently supported SL keywords are:

NumDimensions: A stencil may have 1, 2, or 3 dimensions.

StencilSize: The size of the stencil in each dimension. If the stencil size is 1 in the x dimension, then the value of the cell at (x, y) may be based on the previous iteration's values of the cells in the $x - 1$ and $x + 1$ coordinates.

DataType: The value may be any valid integral type in the target language.

FunctionName: The name of the function that will be exported from the generated source file. The first argument to the function, `data`, will be a matrix of the specified data type with the specified number of dimensions. As input to the function, `data` must contain the initial state of the problem. It must contain valid data in each cell. As output from the function, it will contain the final data. The next n arguments to the function are the input sizes in each dimension. The next argument is the number of iterations to run.

ScalarVariables: A list of numeric variables that will be arguments to the exported function after `data, x, y, z, iterations`. The caller will pass these arguments to the function, and then the stencil calculator will be able to use these variables (read-only) in its calculations.

CellValue: A block of code that will be run for every cell in the data set in every iteration. The code has access to the following variables and functions:

- **x, y, z:** Coordinates of current cell in each dimension.
- **iteration:** Iteration number. Iteration 0 is given as input, so this code will first be called with `iteration`=1.
- **input_size:** a structure with `x`, `y`, and `z` fields, containing the total size of the input
- **the ScalarVariables:** All variables listed in the **ScalarVariables** field.
- **get(...):** a function that efficiently returns data from the stencil from the previous iteration. The parameters are relative to the current cell. For example, in a 2D stencil, the west and east neighbors can be retrieved with `get(-1, 0)` and `get(1, 0)`.
- **read(...):** a function to access read-only data (see below).

The block of code returns the new cell value.

EdgeValue: A block of C code that returns the cell value of cells that are outside the bounds of the input. This code has access to the same variables as the **CellValue** code. Note that at least one of `x`, `y`, or `z` will be out of bounds. This code may not use the `get()` function. Instead, it can access the `value` variable, which will contain the value of the nearest cell in bounds from the previous iteration.

ConvergeScalarVariables: A list of variables passed to the exported function after **ScalarVariables** to specify convergence criteria.

ConvergeValue: A block of code to calculate convergence. This code has access to all of the data and functions available to **CellValue**. Additionally, it has access to the `getNew()` function, which returns the current value at the specified location. **ConvergeValue** is called every PH time steps when desired.

ConvergeType: `ALL` or `ANY` specify that convergence has occured when all or any of the cell values have converged as calculated by **ConvergeValue**.

C. Read Only Data

The generated source file exports two functions. One has the specified function name. The other is called by the specified function name concatenated with `SetData`. For example, if the stencil language file contains the line "`FunctionName runStencil`", then the generated source file will export the functions `runStencil()` and `runStencilSetData()`. The *SetData* function takes two arguments: an array of elements of the specified data type; and the number of elements in the array. If a program calls `runStencilSetData()` with an array, and then calls `runStencil()`, then the stencil calculator will have read-only access to the data in the array. The **CellValue** code can access the i^{th} read-only data element by calling `read(i)`.

V. Stencil Language Compiler

We implemented the stencil language compiler in fewer than 600 lines of Java code. The compiler operates as follows:

1) Converts a stencil language file into a token stream
2) Parses the token stream into a symbol table
3) Reads a plain text template file
4) Outputs a new file which contains the template integrated with the stencil description

This design can easily support multiple architectures and optimizations. We have written templates for CUDA, OpenMP, and MPI code for 1D, 2D, and 3D stencil calculations. Furthermore, the use of a template metaprogramming paradigm does not limit us as, say, a C++ template would; implementing Fortran templates is no more difficult for an experienced Fortran developer than implementing CUDA templates for an experienced CUDA developer. Templates are written such that source code key-value pairs, such

as the **CellValue** pair, have their code can be dropped-in unmodified; thus, given a Fortran template, a Fortran SL program will need to contain valid Fortran code, but will otherwise require no modification. Template code is optimized for shared memory usage, and it calculates the optimal PH. We have also written a template that does not use shared memory or GZs to compare its performance as a naïve CUDA implementation to that of the optimized templates. Our existing, optimized CUDA templates, as used in the evaluation sections of this paper, essentially constitute *hand-optimized code* by any sense of the term.

VI. Generated CUDA Code

The following subsections describe the CUDA architecture, and the details of the SL CUDA template and optimizer.

A. CUDA Architecture Overview

The CUDA programming model [2], [3] is a set of extensions to C and C++ that facilitate the use of NVIDIA GPUs for general-purpose parallel computing. An overview of the NVIDIA Fermi GPU [7] architecture is shown in Figure 4. The model treats the GPU as a parallel co-processor. A control thread on the CPU does some of the work for the application, but can call on the GPU to perform parallel computation when desired. GPU kernels usually represent an inner loop that exhibits large degrees of data parallelism. Kernel code is written for one thread as if it were the only thread running, except that it is given a thread-id from which it can compute its position in the collection of threads launched in the kernel invocation. While kernel code can be written rather simply for simple applications, achieving optimal use of GPU resources is complex and taxing.

One source of complexity in optimizing kernels comes from the specialized GPU memory hierarchy, an artifact of its primary use as a graphics accelerator. GPU hardware is organized into a collection of PEs each of which contains a SIMD core with 8 scalar processing elements. Both the organization of the GPU into separate PEs, and the related variety of different types of memory, are made visible to the CUDA programmer.

When calling a kernel, the user must specify the organization of threads into thread blocks. Tesla GPUs support up to 512 threads per block; Fermi supports 1024. A thread block will be allocated by the CUDA runtime system to a particular PE on which it will execute. To minimize SIMD overhead, these threads are collected into smaller groups called *warps*. Each PE has a modest amount of very fast programmer controlled scratchpad memory, denoted *shared memory*, which can be shared by threads in a thread block but cannot be accessed by any other thread blocks. For the purposes of this paper, the only other memory structure available to threads running on the GPU is a large global memory accessible by all threads on the device.

The CUDA model does not support any global synchronization primitive between thread blocks during a kernel

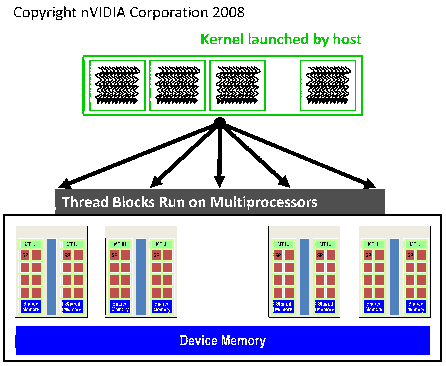

Figure 4. NVIDIA GPU Diagram. The CPU control thread launches a kernel with many threads per thread block. Each thread block is assigned to a Multiprocessor (PE) containing 8 scalar processing elements and a local shared memory. The Device Memory is global to all thread blocks; in pre-Fermi GPUs it was uncached.

execution. Instead, global synchronization events require the completion of all running thread blocks and a return of control to the CPU control thread. A further complication is that no data stored in the shared memory of a PE is persistent across kernel calls. Global synchronization events are therefore very costly.

The implication of this model for stencil applications is that the kernel author must be intimately familiar with the details of the CUDA runtime system in order to organize work units into thread blocks in such a way that usage of shared memory is maximized, and accesses to global memory are minimized. Key decisions in this allocation are the choice of tile size and PH of the stencil calculation that the optimization model is designed to make. In order to accurately make such decisions, the allocator must be able to predict the latencies of the various operations involved in the kernel's calculations and memory accesses.

B. SL CUDA Template

In this section, we describe how our CUDA template code works. This template code is hand-written and hand-optimized by the SL implementers and does not contain any application specific code. The application specific code from the SL specification is automatically merged into the template during the SL translation process to generate the final ISL code. The CUDA execution model involves both a control thread on the CPU and kernel code that executes on the GPU. The CUDA template code includes both the CPU and GPU code needed to support the application specific code provided by the SL user.

The primary function in the template is a C function for the CPU control thread. First, it calculates the tile size and the PH. Then, it copies the input matrix from system memory to GPU memory. If an array of read-only data is used, it also copies that data into GPU memory. Finally, it runs a loop in which it invokes the CUDA kernel to calculate the output matrix from the input matrix. It runs this loop

for the specified number of iterations, divided by the PH, or until convergence as determined by the execution of the **ConvergeValue** code block.

Each tile is processed by one CUDA thread block, and each cell in the tile is owned by a single thread. The input tile size will include GZ cells. The output tile size will be smaller. The actual tile size used is determined at application runtime using dynamically gathered information about the execution environment. For concreteness, consider a pre-Fermi CUDA card that supports up to 512 threads per thread block. In this case, the 3D input tile will be $8 \times 8 \times 8$, the 2D tile 22×22, and the 1D tile 512 cells long.

The generated CUDA kernel includes both template code and application specific code. It operates as follows. The thread calculates the (x, y, z) coordinates of the cell in the matrix that it owns. It copies that cell's value from the input matrix into the thread block's shared memory. After each value has been copied into shared memory, the threads that own cells in the outermost GZ sleep. Those threads have completed their work. Each other thread calculates the new value for its cell. For each cell in its stencil, the thread gets the cell value from shared memory.

If the PH is greater than one, then the threads continue running. Each thread copies the value that it just computed into shared memory. Then, the threads in the second outermost GZ sleep. Their local copies of the neighboring cell values in the outermost GZ are now out-of-date as their values were calculated in an adjacent tile (see Figure 2). The remaining threads calculate new values. This process continues for the number of iterations specified by PH.

When this process is complete, if a thread owned a cell that was not in the GZ, then that cell copies the final value into device memory. If a thread owned a cell that was in the GZ, then that thread does not need to do anything, since we are guaranteed that some thread in some other thread block owned that same cell as part of its output tile, and that other thread will own the responsibility to write the value into device memory.

Inside of the CUDA kernel, the program calls the user-specified **CellValue** code to calculate new cell values, and it calls the user-specified **EdgeValue** code to get stencil values for cells along the edges of the matrix. All of the remainder of the kernel code is included in the template in the SL template library.

C. Pyramid Height Calculation

As mentioned above, the performance of stencil applications on parallel hardware is critically dependent on the proper relationship between tile size and GZ size or PH. To calculate the optimal PH, we extended and automated the CUDA analytical model by Meng and Skadron. They developed a complex analytical model in MatLab that uses information from several sources to calculate the expected program runtime. Their model requires several pieces of information as input.

First, it needs information about the stencil application itself. Some information is static, such as the data dimensionality, the stencil size (GZ), the number of global memory accesses required during movement of tile data into shared memory, and the number of global accesses for read-only data required during each cell calculation. Other information is dynamic, such as the data set size and the number of instructions that each thread must execute in the shared memory setup portion of the kernel and in the kernel cell calculation. Since they proposed but did not implement any code annotations for the stencil applications, many of the application specific parameters were hand coded in MatLab for the four particular test case applications. In addition, the instruction count was gathered using the CUDA profiler on hand-coded implementations of the test applications, and fed to the model by hand.

Second, the specific properties of the target GPU are important. This includes the number of PEs, the number of concurrent blocks that can run on a PE, the number of threads allowed per block, the time required for the GPU to perform a global synchronization, and several GPU memory performance parameters. These values were acquired by a number of means, including hand coding some parameters based on the published characteristics of a few specific models of GPU and by data regression of the runtimes from specific applications.

The multi-node implementation using MPI and CUDA uses the stencil size to determine the necessary border for each node. While this correlates with the concepts of the GZ and PH at the macro level, it is actually statically calculable and does not impact the PH computation. MPI sends the needed data for the assigned elements to the relevant nodes. Nodes return only the calculated results to the root, which collates them to form the result matrix.

1) Modification of Meng and Skadron Model: We have modified and improved this model in several important ways.

First, we ported the model from MatLab to C++ to include it in the application and allow it to perform the optimization at runtime. This allows gathering runtime information about the program in the current execution environment, allowing it to be run on different GPUs without recompilation. The resulting code is better optimized for the specific characteristics of the particular hardware, not just the architectural features of the hardware. While this means that the time to perform the optimizations is included in the total runtime for the program, the difference in runtimes for the wrong optimizations will generally dwarf the cost of calculating the optimizations themselves. In addition, stencil applications typically take many iterations to converge, allowing more time over which to amortize the optimization costs.

Second, the static and architecture-independent application specific information about the dimensions of the data space, the stencil size, etc., now come directly from the SL program specification. These are compiled into the generated code for the ISL calculation.

Third, the remaining application-specific information is acquired dynamically at runtime. This includes the data set size, and the parameters that previously came from profiling, such as the kernel thread setup time and cell value calculation time. The latter two numbers are acquired by running the application with PH of 1 and 2. From these numbers, the setup and cell calculation times are easily computed. Currently we throw away the application computation performed during these data gathering runs, but in the future, the time spent gathering this information could result in the completion of the first three iterations of the computation.

Fourth, the GPU device information is gathered through calls to various functions provided in the CUDA runtime libraries. In particular, we can acquire the number of PEs, the concurrent blocks per PE, and the maximum number of threads per block. We can also query the CUDA runtime system for the number of threads per block for the actual kernel of the running application. This can sometimes result in tighter restrictions on the allowed threads per block if, for example, the kernel requires more resources from the device than the architecture can provide. This is particularly true for CUDA kernels that use many of registers. Knowing this information is critical to optimization because, on the CUDA architecture, stencil applications generally run faster with a larger tile size as long as the data set size is large enough to saturate the number of available PEs. Since the threads-per-block count determines the tile size, knowing this number precisely allows the optimizer to pick the largest tile size that the current GPU can handle. Future GPUs will likely allow the number of threads per block to increase further; gathering this information at run time allows generated code to calculate the optimal tile size for such cards without recompilation.

Fifth, the time required for a global synchronization is acquired by running a null kernel on the device with the same data set size parameters as are required to run the actual kernel.

Finally, Meng and Skadron originally did a manual gradient descent on runtimes to determine the best PH and tile size. Since we can determine the best tile size as described earlier, we do an automatic gradient descent starting at PH of 1, and continue calculating the model latency until it is higher than the previous one, then use that PH for the remainder of the application iterations.

VII. Experimental Results

Our primary emphases are the definition of a stencil language, providing a source-to-source compiler for it, and optimizing the generated programs in terms of GPU shared memory, tile size, and PH with an extension of the analytical model of Meng and Skadron. The availability of the Fermi and Tesla architectures presents an opportunity to test the robustness to architectural changes of our model enhancement which utilizes dynamically-collected information about the execution environment. Therefore, we present results for a GTX 480 (Fermi) and a GTX 280 (Tesla).

All runtimes include the CPU and GPU latencies for the ISL loop only. The time required to create and initialize arrays, and transfer arrays between main memory and the GPU global memory are not included to allow us to focus on the factors affecting the ISL performance. In addition, the reported runtimes for the SL optimized ISLs do not include the overhead needed to run the optimizer. Instead, the times are for the entire ISL loop running with the parameters determined by the optimizer. As stated above, the costs for running the optimizer are fixed, so the overhead for the optimizer as a percentage of the overall runtime can be arbitrarily large or small depending on the number of iterations in the actual ISL loop.

We use the arithmetic mean when aggregating results and a SERPOP analysis strategy (see [8] for details).

Our GTX 480 is in a machine with an Intel Core2 Quad Q9400 clocked at 2.66 GHz with 3 MB L2 and 4 GB DRAM running Linux 2.6.32. The 280 is attached to dual Intel Core2 Extreme X9770 processors running at 3.2GHz with 6MB of L2 cache and 4GB of DRAM running Linux 2.6.24. Both machines are running CUDA 3.1. The 480 can manage 1024 threads per block with 60 PEs each with 8 SIMD cores running at 1.4 GHz. It has 2 GB of memory. The 280 has 30 PEs, each with 8 SIMD cores that handle up to 8 concurrent running blocks with a 512 thread maximum block size. It is clocked at 1.3 GHz with 1 GB of global memory. All code was compiled with the NVIDIA NVCC compiler which calls GNU tools (version 4.2.4) for compiling C++ code and linking. All code was compiled with -O3. Our generated optimized code is based on hand optimized templates, and thus is essentially equivalent to hand optimized code.

For our first test cases, we use the same four stencil applications as Meng and Skadron did in their original study. They are described below. All of the graphs of runtimes versus PH have the same basic curve. Very low PHs are not large enough to take advantage of all available spatial and temporal locality, and perform worse than larger PHs, especially given the relatively large cost of global synchronizations in the CUDA architecture. However, beyond some optimal PH, the runtimes again increase due to the overhead of the redundant local GZ value calculations. Another way to view this trade-off is that with increased PH, the number of threads per tile that calculate final cell values drops off at twice the size of the stencil per dimension per step in PH (see Figure 2); therefore, for larger PHs the effective tile size gets smaller, and the total number of tiles—and therefore also the total number of threads—increases. Eventually, in the limiting case, the PH is so high that *no* useful cell values are calculated. For these reasons, all of the graphs of runtimes versus PH will be bowl shaped. To better highlight the important portions of the curves near the optimal—the minimum of the respective curve—PH, in the following graphs we have not shown the extreme values at very high

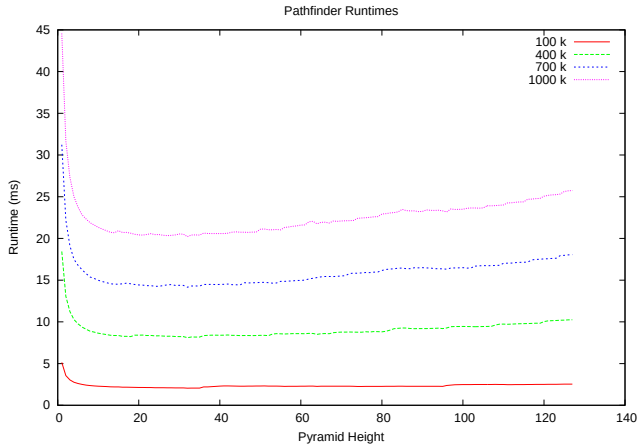

Figure 5. Fermi runtimes for the Pathfinder 1D application versus PH. The lowest portion of the curves are very flat. Therefore, even though our model did not pick the optimal PH for any data set size, performance was still near optimal.

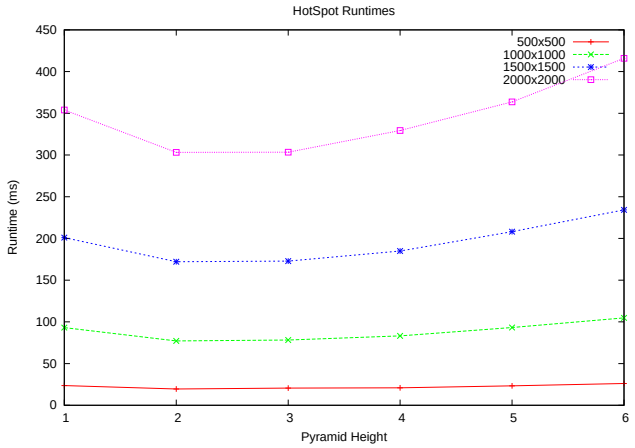

Figure 6. Fermi runtimes for the HotSpot 2D stencil application versus PH. As can be seen, the curve is bowl shape with a minimum at PH 2. The effect is more pronounced with greater data set sizes. Our optimizer picked the correct PH of 2 for all these data sets.

PH. Furthermore, we present results for both the Fermi and Tesla architectures; however, as the results are generally quite similar, we only include graphs for Fermi. Differences in results are discussed in the text.

A. "Pathfinder"

The first test case is a 1D stencil application called *"Pathfinder"* that performs a dynamic programming calculation of the lowest cost of any vertical path through a 2D grid. The 2D input data set is read-only data in the **CellValue** computation. Each loop iteration calculates the minimum costs down another row in the 2D grid. The tiles are horizontal slices across the columns of the grid. A valid path is one which varies by at most one cell in each step from row to row, thus the stencil size is 1. Figure 5 shows the Fermi runtimes versus PH for Pathfinder for row widths of 100 k, 400 k, 700 k, and 1000 k. As with all the applications, these large sizes are chosen to ensure that the GPU is computationally saturated. The PH can range from 1 to 255 on Tesla and 1 to 511 on Fermi.

Notice that the valley for the main portion of this curve is very shallow. Therefore, it is hard for the model to accurately predict the exact best PH. And in fact, our model does not. The measured best PH is 16 for all data set sizes. However, our optimizer predicts 61, 24, 24, and 25 for the 100 k, 400 k, 700 k, and 1000 k data set sizes and resulting in performance loses of only 12%, 2.6%, 0.7%, 1.2%, respectively. Tesla results are similar, with a performance loss of 5.8% for the 400 k dataset and less than 1% for all others. From these results, one can see that the shape of the interesting part of the curve is so flat that precise PH prediction is not necessary to achieve very positive results. For comparison, the poor choice of a PH of 1 for the 400 k column data set would result in a performance loss of nearly $2.5\times$.

B. "HotSpot"

The second test case is a 2D stencil application called *"HotSpot"*. The stencil language description for this application is shown in Figure 3. The application solves a series of ordinary differential equations that model heat dissipation in a conductive material, the silicon substrate of a computer chip [9]. On each time step of the computation, the heat generated by the chip components propagates through the modeled substrate. This is constant read-only data read for each cell on each iteration. As this is a 2D application, the theoretical maximum square tile size on a Fermi board is 32x32, and 22x22 on Tesla implying possible PH ranging from 1–15 and 1–10, respectively. The Fermi runtimes versus PH are show in Figure 6. As can clearly be seen, for the four data set sizes, the optimal PH is 2; this also holds true for Tesla. That is also the height calculated by our optimizer.

C. "Plate"

The third test case is a 2D stencil application called *"Plate"*. It is very similar to and replaces the *"Poisson"* application from the original test suite. It also models heat transfer in a plate but this time, the heat injection into the system is modeled as coming from the edge of the plate, not distributed throughout. This differentiates the application from HotSpot in two important ways. First, there is no required read of global data in each time step. Second, it gives us an opportunity to use the **EdgeValue** capability of SL to inject the heat at the plate's edge. Again the maximum square tile sizes are 32x32 and 22x22 and valid PHs are 1–15 and 1–10 for Fermi and Tesla, respectively. The Fermi model predicted optimal PHs of 4, 3, 3, and 3 for the 500^2, 1000^2, 1500^2, 2000^2 stencils, respectively, and the Tesla model predicted optimal PH or 2 across the board. All predictions were accurate. As the results for Plate are so similar to HotSpot, we don't include a graph.

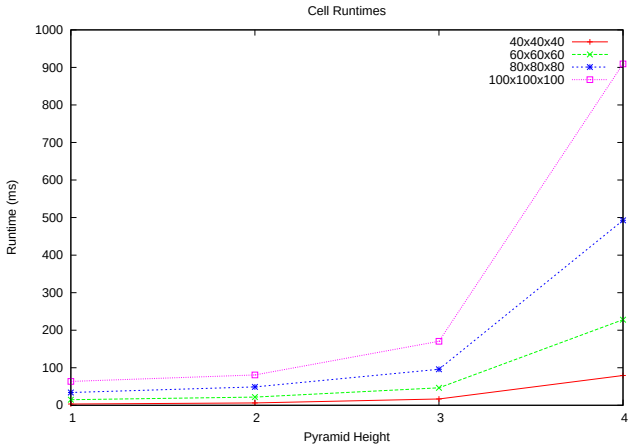

Figure 7. Fermi runtimes for the Cell 3D stencil application versus PH. The curve shows that a PH of 3 or 4 is a very bad choice. While the values for 1 and 2 are slightly compressed in the graph, the optimal PH is in fact 1 for all data sets.

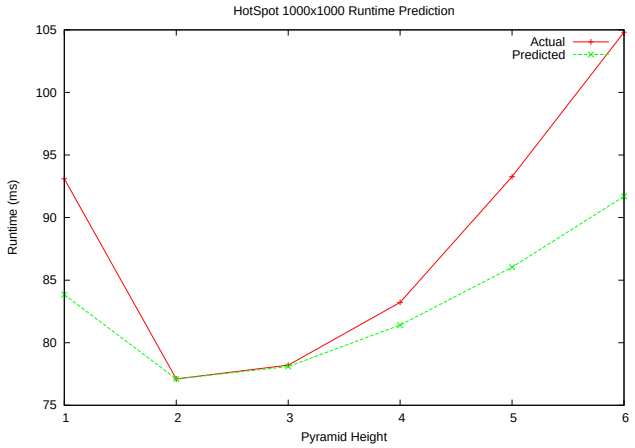

Figure 8. Fermi runtimes for HotSpot versus normalized runtimes predicted by the Model for PHs from 1 to 6. While the shape of the model curve does not precisely match that of the measured runtimes, the model accurately predicts an optimal PH of two.

D. "Cell"

The fourth test case is a 3D stencil application called *"Cell"*. It models Conway's Game of Life in 3 dimensions. In each time step, each cell calculates whether it is alive or dead based on the number of neighboring cells that were alive in the previous time step. To perform this calculation, it looks at its 26 nearest neighbors. For a 3D application, the maximum tile size on Tesla is 8x8x8, and 10x10x10 on Fermi, and the possible PHs are only 1–3 and 1–4, respectively. The Fermi runtimes versus PH are shown in Figure 7. It is clear from the chart that a PH of 3 or 4 is a very bad choice. The runtimes for PHs of 1 and 2 are similar, but 1 is better and is also correctly predicted by our model in all cases for Tesla and in all but the 40^3 case on Fermi, which predicted an optimal PH of 2.

E. Model Comparisons

As we have demonstrated, our model predicts the optimal PH for HotSpot, Plate, and Cell (save one instance out of eight) on Fermi and Tesla. These were the same PHs predicted by the original model of Meng and Skadron for these same applications and data set sizes; however, they measured an optimal PH of 3 for HotSpot and Poisson. Their implementation differs from ours in two important ways.

First, their implementations took advantage of architectural details that are not exposed to users of SL, allowing them to load the read-only heat data used in HotSpot into shared memory to take advantage of temporal locality. Our SL has no way for the application programmer to express the access patterns for read-only data, and therefore our version of HotSpot will read the value from global memory in each time step. The ability of hardware-tuned code to reuse the global memory read across several time steps tends to drive the optimal PH higher, leading to greater temporal reuse of data values loaded into shared memory. We hope to add better support for read-only data to SL at a future date.

Second, their inner loop code calculates the cell values for all cells in the tile, even those that have become too far away from the center of the tile to matter to the computation. Another option is to recalculate the zone of cells involved in useful computation on each time step. This keeps threads from calculating values that will never be used at the cost of more GZ size calculations. Given that our system must access read-only data from global memory in HotSpot—and potentially in other applications—the strategy of recalculating the GZ size in each time interval mitigates the number of global reads required, and is therefore the correct choice for such applications.

We found that 2D and 3D applications run faster by restricting the number of calculated values, even without using read only data. We believe this is because whole thread warps on the top and bottom of the tile will only have to check on each time step if they are still calculating useful values. In 3D applications, this effect is even more pronounced as warps in the front and back of the tile have this same advantage. The GZs on the sides of the tile tend not to span entire warps, so there is no advantage for warps at the sides of the tile from this effect, while the GZs in a 1D application only grow on the sides. Our CUDA templates take advantage of these effects by continuing to calculate values in the GZ for 1D stencil applications, but not for 2D or 3D applications. As a result of this change, our Pathfinder runtimes were significantly reduced.

We also analyzed the actual runtimes versus our model predictions. Figure 8 shows HotSpot runtimes on Fermi versus predictions for PHs from 1 to 6. The model predictions are in terms of GPU cycles, not runtimes. Therefore, the model times are normalized to the actual runtime at the optimal PH of 2. This allows a more direct comparison of the relative curves shapes, which is more important than absolute scaling for choosing the optimal PH. As the figure shows, the model has a steeper bowl shape than the actual runtimes. The effect is more pronounced for higher PHs,

Application	Pathfinder	Plate	PlateHalo	Plate++	HotSpot	Cell
Fermi						
Data Set Size	400K	1000^2	1000^2	1000^2	1000^2	60^3
Source of Best Time	O PH=32	SL PH=3	SL PH=3	SL PH=2	SL PH=2	SL PH=1
Oracle	8.3 ms	61.4 ms	66.7 ms	85.9 ms	78.0 ms	16.0 ms
SL Optimized vs Naïve	2.06	1.17	1.54	1.26	1.11	1.44
SL Optimized Time	8.6 ms	61.4 ms	66.7 ms	85.9 ms	78.0 ms	16.0 ms
SL PH=1	18.4 ms	81.3 ms	85.1 ms	91.9 ms	95.8 ms	16.0 ms
Naïve	17.7 ms	71.8 ms	102.8 ms	108.0 ms	86.3 ms	23.0 ms
Tesla						
Source of Best Time	O PH=16	SL PH=2	SL PH=2	SL PH=1	Naïve	SL PH=1
Oracle	9.4 ms	114.2 ms	131.8 ms	176.3 ms	141.0 ms	36.5 ms
SL Optimized vs Naïve	2.37	1.09	1.82	1.26	0.97	2.37
SL Optimized Time	9.7 ms	114.2 ms	131.8 ms	176.3 ms	145.3 ms	36.5 ms
SL PH=1	23.6 ms	145.1 ms	160.1 ms	176.3 ms	162.9 ms	36.5 ms
Naïve	23.0 ms	124.9 ms	239.7 ms	222.0 ms	141.0 ms	86.6 ms

Figure 9. Runtimes for the SL optimized code for the four applications in Section VII, plus two new versions of Plate. Runtimes are also shown for a naïve CUDA implementation, along with a comparison relative to SL optimized code. For applications with large amounts of either temporal or spatial locality, the SL generated code far outperforms the naïve code. For other applications, the difference is more modest. Data are listed for Fermi, on the top of the table, and Tesla, on the bottom. Fermi's larger block size results in higher optimal PH for Plate, PlateHalo, and Plate++ due to the larger tile sizes. The inclusion of a cache on Fermi also results in a lower relative improvement of SL optimized code versus naïve for applications with large amounts of temporal or spatial locality.

and grows large quickly for PHs between 6 and 10 which are truncated to better show the most interesting part of the curves.

The results presented here validate that the changes that we have made to the CUDA ISL analytical model have not lessened the effective accuracy of its PH predictions. Given the advantage of the elimination of the users' manual involvement in this optimization, we believe this to be an important contribution of this work.

F. Comparison to Naïve CUDA code

In judging the performance of optimized code, it is important to see the effects of the optimizations compared against code that does not have those optimizations. Table 9 shows where we compare a "naïve" CUDA implementation of the four applications discussed above along with two additional applications.

The naïve CUDA implementation does not use shared memory. Instead, global device memory is always accessed. Therefore, each PE can only calculate one time step before synchronizing with neighboring PEs. While there are some edge cases to consider at the boundaries of the data set, there is no longer any need to handle edge cases across internal tile boundaries. The naïve code does still benefit from large tile sizes; the maximum possible sizes are used. Overall, this code is much simpler than the optimized code, and approximates what an inexperienced CUDA programmer would produce.

The also shows the runtimes of the SL generated code, but with PH=1. Finally, the table also shows the runtime of the SL generated code with an oracle selecting the best code. This often matches the SL optimized code, but differs in those cases where SL does not accurately predict the best PH, and the one case where the naïve code outperforms the SL generated code.

We can see from the table that the SL generated code outperforms the naïve code by between $2.37\times$ and $0.97\times$ with an arithmetic mean of $1.65\times$. The SL optimized code outperforms the naïve code by a significant factor for both the 1D Pathfinder application, and the 3D Cell application, but for different reasons. In Pathfinder, the optimal PH are high at 32 and 16, so there is substantial temporal reuse of the data values stored in shared memory even though the spatial reuse is limited by the single dimension of the data. This is further seen by looking at the PH=1 runtime for the SL code. By setting the PH=1, all of the temporal reuse is eliminated, and the overhead of the additional complexity of the SL code causes it to run slightly slower than the naïve code.

On the other hand, in Cell, the stencil involves 26 neighboring cell values. So, even though the temporal reuse is non-existent with an optimal PH of 1, the spatial reuse is significant. In the 2D applications, the optimal PH of Plate and HotSpot are always small, and the stencil involves only 4 adjacent cells, so neither the spatial nor temporal reuse is extremely high. In fact the naïve code runs faster than SL's optimal code for HotSpot on Tesla, as the latter is also doing global memory reads in each time step.

To further explore these issues, we added two additional versions of Plate to our study. The first,*PlateHalo*, expands the number of adjacent cells used in the computation to 8 by including the diagonal neighbors. This increases the spatial locality of the data in shared memory, and we see that the runtime for the naïve version increases significantly in PlateHalo over Plate, while the SL optimized version shows only a modest change in performance.

The second variation of Plate is called *Plate++*. It also expands the stencil to include 8 neighbors, but this time by going out 2 cells to the north, south, east, and west. As this causes the GZs to grow twice as fast as in Plate, the optimal PH are now 1 and 2. Temporal reuse is reduced—eliminated on Tesla—in the SL code, and SL code for Plate++ runs slower than either Plate or PlateHalo. The naïve code for Plate++ runs 8% faster than the naïve code for PlateHalo on Tesla, perhaps because of better memory access coalescence, or fewer memory bank conflicts.

G. Multinode CUDA with MPI

Our MPI implementation does not account for non-heterogeneous distribution of GPUs, nor do we have machines with matching hardware such that we can do a complete, fair performance evaluation of a multinode GPU cluster. We present multinode results to show proof of concept and that even a naïve multinode implementation on a non-heterogeneous cluster will provide performance benefits.

Figure 10 shows the speedup of a heterogeneous 2-node cluster over it's constituent nodes, one running a GTX 460 and the other a Tesla C2050. The figure also shows the speedup of the 2050 over the 460 to give an idea of the relevant performance differences of the parts. Other benchmarks demonstrate similar results. This figure shows that optimal pyramid height is independent of multinode

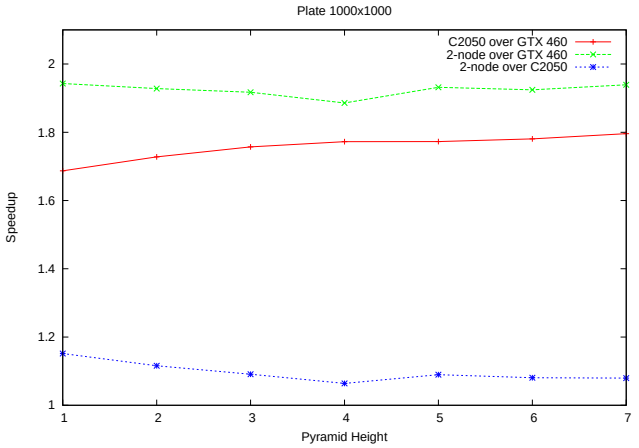

Figure 10. 2-node performance for Plate at 1000×1000 using a GTX 460 and a C2050. The speedup for the C2050 over the GTX 460 is also included to give a sense of the performance differences of the parts.

computation, at least until working sets become so small that communication dominates.

VIII. Related Work

Li et al. may have been the first to use the term *iterative stencil loops* [1]. They developed a compiler framework for these loops that used tiling to improve temporal data locality. Their work was intended to be run on a uniprocessor, so they did not face any communication costs and they did not consider ghost zones.

We are not the first to create a stencil compiler. Brickner et al. created a stencil compiler for the Connection Machine CM-2 massively parallel architecture [10]. The stencil expression was expressed in microcode which was specific to the CM-2. Other recent stencil compilers are Pochoir [11] and PATUS [12]. Our framework is distinguished from these by the inclusion of MPI and by our runtime optimizations.

In parallel with our efforts, Orchard et al. [13] have developed a stencil language called *Ypnos* as an extension to Haskell. They also argue for an architecture-independent declarative language for ISLs, and as in SL, rely on language features instead of complex program analysis to determine the size and shape of the stencils and data. Their language includes reduction operators as a means of specifying convergence criteria, and they allow users to explicitly specify a PH for an ISL computation but do not support automatic PH optimization. They do not report Ypnos performance results.

Kamil et al. [14] studied the effects of tile size and time skewing on memory locality on Itanium2, Opteron, Power5, and Cell. They concluded that controlling tile size, temporal locality across time slices, and hand-tuned control of scratchpad memory is critical to performance. We optimize use of CUDA's scratchpad memory, tile size, and temporal reuse; however, our temporal locality is always strictly in the time dimension, as we have not investigated the use of time skewing. Datta et al. [15] studied optimizations for stencil applications across a wide range of architectures including CUDA. Their optimizer uses auto-tuning to find optimal solutions, as does another paper by Kamil et al [16]. Our analytical model starting point allows our training period to be very short relative to a typical ISL computation.

Micikevicius explored hand coding stencil applications for CUDA, and ghost zone sizes [17]. They also explored using asynchronous data transfers for data sets too large to fit in GPU global memory. Volkov et al. explored hand optimizing CUDA programs involving parallel operations on large arrays [18]. We have included a subset of the optimizations presented by Micikevicius and Volkov in our CUDA template library, but we have no support for arrays too large to fit into the device's global memory, and therefore we did not investigate asynchronous data transfers.

Several attempts have been made to build simplifying layers on top of CUDA. Lee et al. implemented a source-to-source translator for OpenMP to CUDA [19]. OpenMP can express a significantly wider range of parallel computations then can be expressed by SL; however, this also means an OpenMP translator cannot include stencil application specific optimizations as we do. There is also previous work similar in nature to the pyramid height optimization including work by Bassetti et al. [20] and Nguyen et al [21].

CUDA-lite is a general purpose, source-to-source translator for automatically optimizing CUDA programs [22]. The user specifies a naïve CUDA implementation of their ISL that only uses global memory, and adds some pragmas that give hints about the size, shape, and data access patterns. Then CUDA-lite generates an optimized CUDA program that leverages the specialized memory spaces, resulting in 2–17$\times$ speedups for their test applications. It appears they ran their tests on earlier GPUs that had less flexible memory access coalescing hardware than modern GPUs. In addition, their primary test applications were not stencil applications, and instead performed operations such as matrix multiply. These contain large amounts of spatial and temporal locality, and are compute intensive, allowing for more processing time to hide memory access latency [23]. By comparison, SL also optimizes for shared memory but not texture memory, and also optimizes PH.

IX. Conclusions and Future Directions

We have defined a new language, SL, for easily expressing stencil applications. SL is a formal, high-level language in which a programmer can conveniently describe an ISL computation by focusing on the simple computation needed to compute cell values. No optimization nor architecture-specific information is needed.

We have created an SL compiler that uses templates to allow the generated code to be extended to many parallel execution environments. Based on a single source file, it generates efficient code for CUDA, OpenMP and MPI; other environments are possible. SL's architecture allows targeting of languages which are not C-like; Fortran, for example, which is still quite popular for high-performance computing.

We have implemented an initial template and an optimizer for the CUDA programming environment that blocks

computations to use the scratchpad memory, and that estimates the best PH. The optimizer is fully automatic and utilizes both static and dynamic application information. It accurately calculates the optimal tile size and PHs for most applications, on both Tesla and Fermi class GPUs. As a result, with an SL source of about 16 lines, a user can achieve average speedups of $1.65\times$ for the GTX 280, and $1.43\times$ for the GTX 480, over naïve CUDA code. Yet the SL specification is much easier to write than even the naïve CUDA code, and is similar to writing code for a single thread CPU.

The optimizer's ability to leverage dynamically acquired information about the runtime environment means that the generated code can be used on a variety of devices. Our model ported directly from its original the Tesla target to the Fermi architecture with only trivial modification.

The current SL architecture can be extended in several directions. First, with language extensions, we can improve support for read-only data at least in the common cases, such as HotSpot, where the array access pattern is straightforward. A second SL language extension could add support for reduction operators and ISL termination based on a data convergence criteria. It would also be interesting to investigate data morphing as a way to improve cache performance or reduce memory bank conflicts.

ACKNOWLEDGEMENTS

This work was supported in part by NSF grant CNS-0916908 and by a grant from NEC Research Labs America.

REFERENCES

[1] Z. Li and Y. Song, "Automatic Tiling of Iterative Stencil Loops," *ACM TOPLAS*, vol. 26, no. 6, pp. 975–1028, 2004.

[2] E. Lindholm, J. Nickolls, S. Oberman, and J. Montrym, "NVIDIA Tesla: A Unified Graphics and Computing Architecture," *IEEE Micro*, vol. 28, no. 2, pp. 39–55, 2008.

[3] J. Nickolls, I. Buck, M. Garland, and K. Skadron, "Scalable Parallel Programming with CUDA," *Queue*, vol. 6, no. 2, pp. 40–53, 2008.

[4] B. Chapman, G. Jost, and R. v. d. Pas, *Using OpenMP: Portable Shared Memory Parallel Programming (Scientific and Engineering Computation)*. The MIT Press, 2007.

[5] MPI Forum, "MPI: A Message-Passing Interface Standard. Version 2.2," September 4th 2009, available at: http://www.mpi-forum.org (Dec. 2009).

[6] J. Meng and K. Skadron, "Performance Modeling and Automatic Ghost Zone Optimization for Iterative Stencil Loops on GPUs," in *23rd International Conference on Supercomputing*, 2009, pp. 256–265.

[7] J. Nickolls and W. Dally, "The GPU Computing Era," *IEEE Micro*, vol. 30, no. 2, pp. 56 –69, March-April 2010.

[8] J. R. Mashey, "War of the Benchmark Means: Time for a Truce," *SIGARCH Computer Architecture News*, vol. 32, no. 4, pp. 1–14, 2004.

[9] K. Skadron, M. R. Stan, K. Sankaranarayanan, W. Huang, S. Velusamy, and D. Tarjan, "Temperature-Aware Microarchitecture: Modeling and Implementation," *ACM TACO*, vol. 1, no. 1, pp. 94–125, 2004.

[10] R. Brickner, W. George, S. L. Johnsson, and A. Ruttenberg, "A Stencil Compiler for the Connection Machine Models CM-2/200," in *Fourth Workshop on Compilers for Parallel Computers*, 1993.

[11] Y. Tang, R. A. Chowdhury, B. C. Kuszmaul, C.-K. Luk, and C. E. Leiserson, "The pochoir stencil compiler," in *SPAA*, R. Rajaraman and F. M. auf der Heide, Eds. ACM, 2011, pp. 117–128.

[12] M. Christen, O. Schenk, and H. Burkhart, "Patus: A code generation and autotuning framework for parallel iterative stencil computations on modern microarchitectures," *Parallel and Distributed Processing Symposium, International*, vol. 0, pp. 676–687, 2011.

[13] D. A. Orchard, M. Bolingbroke, and A. Mycroft, "Ypnos: Declarative, Parallel Structured Grid Programming," in *5th Workshop on Declarative Aspects of Multicore Programming*, New York, 2010, pp. 15–24.

[14] S. Kamil, K. Datta, S. Williams, L. Oliker, J. Shalf, and K. Yelick, "Implicit and Explicit Optimizations for Stencil Computations," in *Workshop on Memory System Performance and Correctness*, 2006, pp. 51–60.

[15] K. Datta, M. Murphy, V. Volkov, S. Williams, J. Carter, L. Oliker, D. Patterson, J. Shalf, and K. Yelick, "Stencil Computation Optimization and Auto-tuning on State-of-the-art Multicore Architectures," in *Conference on Supercomputing*, Piscataway, NJ, 2008, pp. 1–12.

[16] S. Kamil, C. Chan, L. Oliker, J. Shalf, and S. Williams, "An auto-tuning framework for parallel multicore stencil computations," in *Parallel Distributed Processing (IPDPS), 2010 IEEE International Symposium on*, april 2010, pp. 1 –12.

[17] P. Micikevicius, "3D Finite Difference Computation on GPUs using CUDA," in *2nd Workshop on General Purpose Processing on Graphics Processing Units*, 2009, pp. 79–84.

[18] Volkov, Vasily and Demmel, James, "LU, QR and Cholesky Factorizations using Vector Capabilities of GPUs," University of California at Berkeley, Tech. Rep. UCB/EECS-2008-49, May 2008.

[19] S. Lee, S.-J. Min, and R. Eigenmann, "OpenMP to GPGPU: A Compiler Framework for Automatic Translation and Optimization," *SIGPLAN Notices*, vol. 44, no. 4, pp. 101–110, 2009.

[20] F. Bassetti, K. Davis, and D. J. Quinlan, "Optimizing transformations of stencil operations for parallel object-oriented scientific frameworks on cache-based architectures," in *Proceedings of the Second International Symposium on Computing in Object-Oriented Parallel Environments*, ser. ISCOPE '98. London, UK: Springer-Verlag, 1998, pp. 107–118.

[21] A. Nguyen, N. Satish, J. Chhugani, C. Kim, and P. Dubey, "3.5-d blocking optimization for stencil computations on modern cpus and gpus," in *Proceedings of the 2010 ACM/IEEE International Conference for High Performance Computing, Networking, Storage and Analysis*, ser. SC '10. Washington, DC, USA: IEEE Computer Society, 2010, pp. 1–13.

[22] S.-Z. Ueng, M. Lathara, S. S. Baghsorkhi, and W.-M. W. Hwu, "CUDA-Lite: Reducing GPU Programming Complexity," in *21st Workshop on Languages and Compilers for Parallel Computing*, Berlin, Heidelberg, 2008, pp. 1–15.

[23] S. Ryoo, C. I. Rodrigues, S. S. Baghsorkhi, S. S. Stone, D. B. Kirk, and W.-m. W. Hwu, "Optimization Principles and Application Performance Evaluation of a Multithreaded GPU using CUDA," in *Principles and Practice of Parallel Programming*, New York, 2008, pp. 73–82.